A Novel Neutral Point Potential Stabilization Technique Using the Information of Output Current Polarities and Voltage Vector

Katsutoshi Yamanaka, Ahmet M. Hava, *Member, IEEE*, Hiroshi Kirino, Yoshiyuki Tanaka, Noritaka Koga, and Tsuneo Kume, *Member, IEEE*

***Abstract*—This paper proposes a new neutral point potential control technique for the neutral-point-clamped three-level inverter. Utilizing the phase current polarity information, this technique distributes the redundant voltage vectors in a manner to obtain stable neutral point voltage under all operating conditions including the zero-power-factor condition. Detailed analysis and computer simulations show the superiority of the proposed method. The feasibility of the proposed method has been proven via laboratory experiments.**

***Index Terms*—Current polarity, inverter, neutral point potential, space vector, stabilization.**

I. Introduction

THE neutral-point-clamped (NPC) three-level inverter is suitable for medium- and high-voltage drive applications because the voltage stress on its switching power devices is half the voltage stress on the devices of the conventional two-level inverter [1]. Recently, general-purpose pulsewidth-modulated (PWM) NPC three-level inverters have been developed for low-voltage drive applications [2] because the NPC three-level inverter has significantly better output voltage and current waveforms [lower harmonics and less electromagnetic interference (EMI)] than the two-level inverter. Fig. 1 shows the circuit diagram of the NPC three-level inverter.

One important problem associated with the NPC three-level inverter is its neutral point potential variation [3]. Under certain conditions, the dc-link neutral point potential can significantly fluctuate or continuously drift to unacceptable levels. As a result, the switching devices may fail due to overvoltage stress, rendering the drive unreliable.

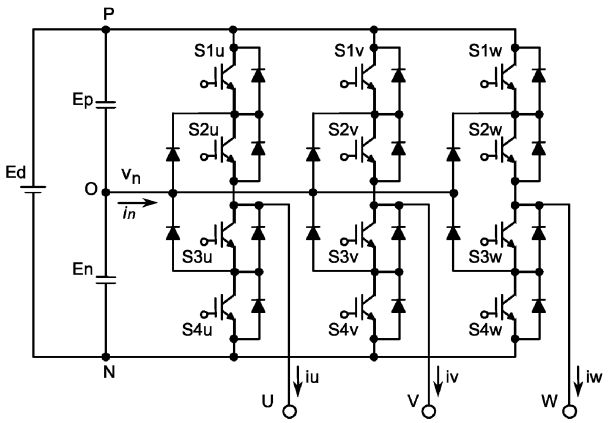

Fig. 1. NPC three-level inverter circuit topology.

The causes of neutral point potential drift can be nonuniform switching device or dc-link capacitor characteristics. Such unbalances can lead to slow but continuous drift of the neutral point potential. Dynamic operating conditions such as acceleration or deceleration can also result in neutral point potential drift. Under such conditions, the drift can be rapid and significant.

The neutral point potential fluctuation involves both the modulation technique and the operating conditions of the NPC. For each modulation technique and neutral point potential control technique involved, the neutral point potential varies differently. However, in most techniques the operating point dependency is similar. As the output voltage magnitude and the load current magnitude increase, and the power factor (PF) approaches zero, the neutral point potential fluctuation increases. Under such operating conditions, the NPC three-level inverter performance degrades and becomes unreliable. Therefore, the choice of appropriate modulation techniques and the development of advanced neutral point potential control techniques is necessary to overcome the neutral point potential problems. Although it is possible to reduce the neutral point potential deviation problem by increasing the dc-link capacitor and the bleeding resistor size excessively, such a solution is prohibitive from the cost and size reduction perspectives.

The neutral point potential variation problem has recently been investigated and several control techniques have been developed [3]–[13]. Although the influence of the load current, PF, and the output voltage magnitude on the neutral point potential is quali-

Paper IPCSD 02–046, presented at the 2001 Industry Applications Society Annual Meeting, Chicago, IL, September 30–October 5, and approved for publication in the IEEE TRANSACTIONS ON INDUSTRY APPLICATIONS by the Industrial Power Converter Committee of the IEEE Industry Applications Society. Manuscript submitted for review October 15, 2001 and released for publication July 22, 2002.

K. Yamanaka and Y. Tanaka are with the Mechatoronics R&D Department, Corporate R&D Center, Yaskawa Electric Corporation, Kitakyushu 803-8530, Japan (e-mail: cutc@yaskawa.co.jp; zenchan@yaskawa.co.jp).

A. M. Hava is with the Electrical and Electronics Engineering Department, Middle East Technical University, Ankara 06531, Turkey (e-mail: hava-hava@yahoo.com).

H. Kirino is with the Inverter Design Section, Motion Control Division, Yaskawa Electric Corporation, Yukuhashi-City 824-8511, Japan (e-mail: kirino@yaskawa.co.jp).

N. Koga is with the Drive Planning Section, Motion Control Division, Yaskawa Electric Corporation, Iruma-City 358-8555, Japan (e-mail: norikoga@yaskawa.co.jp).

T. Kume is with Yaskawa Electric America, Inc., Waukegan, IL 60085 USA (e-mail: Joe_Kume@yaskawa.com).

Digital Object Identifier 10.1109/TIA.2002.804761

tatively understood, the modulation and control techniques that effectively manipulate the variation are not well established. In [3], the scalar unipolar modulation technique has been considered and analytical formulas that calculate the zero-sequence signal for minimum neutral point potential variation were developed. The neutral potential behavior of the scalar bipolar modulation method has not been reported. Although the space-vector-based neutral potential behavior analysis in [10] is comprehensive, it does not lead to a simple/efficient controller development. Furthermore, the relation between the scalar and vector modulation techniques from the neutral point potential control perspective is not well understood. Several recent attempts to provide comprehensive analysis and control techniques have covered a limited scope and shortage of information on the subject remains significant [10], [12], [15], [16]. On the other hand, for the economical feasibility of a general-purpose low-voltage NPC three-level inverter the development of a neutral potential controller with low cost (minimum hardware/software requirements) and high performance is crucial.

In this paper, first the neutral point potential variation is analytically investigated for the space-vector modulation technique. The analysis leads to a simple and high-performance neutral point potential control technique that utilizes the polarity information of the motor phase currents and the space vector redundancy function. In the proposed technique, the redundant voltage vectors are efficiently distributed such that the neutral point current and, therefore, the neutral point potential is controlled under all operating conditions. The neutral potential performance of the proposed method is investigated by analysis and computer simulations. Its performance is also compared to the popular scalar unipolar modulation with zero-sequence signal injection method [3] and its superior performance is shown. The feasibility of the proposed method has been proven via laboratory experiments.

II. Analysis of the Neutral Point Potential Variation

In the space-vector representation, the 27 NPC three-level inverter output voltage vectors can be represented as shown in Fig. 2. As the figure indicates, the small vectors (grouped as (ap, an) and (bp, bn) and the zero vectors (op, oo, and on) are redundant [4], [5]. The medium vectors labeled with "c" and the full vectors (a and b) are not redundant. Only the small vectors with the size of $Ed/3$ and the medium vectors with the size of $Ed/\sqrt{3}$ load the neutral point. Of these, only the small vectors are redundant. Therefore, the only means to balance the neutral point potential is to control the small redundant vectors. If an adequate control technique is not utilized, the neutral point potential can significantly fluctuate or even drift to excessive values, resulting in performance degradation and, furthermore, in semiconductor device failure. In particular, the neutral point potential fluctuation is maximum when operating at the maximum output voltage with near-zero PF [3].

The influence of the small redundant vectors on the neutral point potential is illustrated in Fig. 3. As the figure suggests, when selecting a pair of redundant vectors (ap, an) or (bp, bn), the redundancy ratio must be carefully selected in order to control the average neutral point current flow over the PWM cycle.

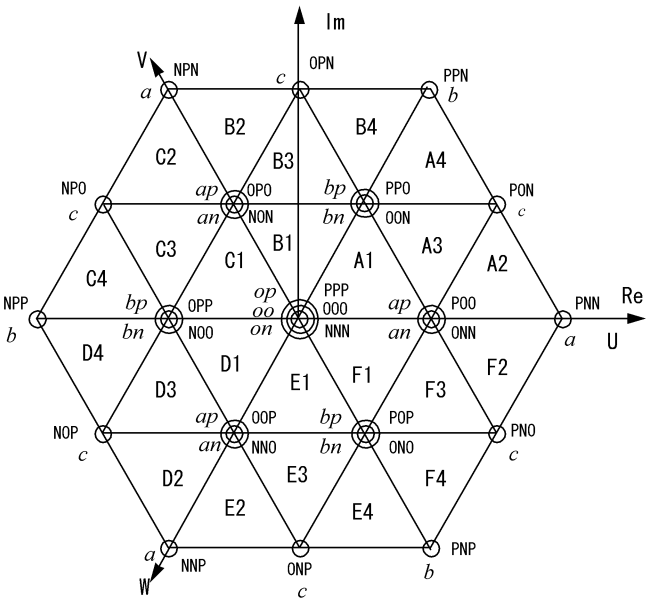

Fig. 2. Space-vector representation of the NPC three-level inverter output voltages.

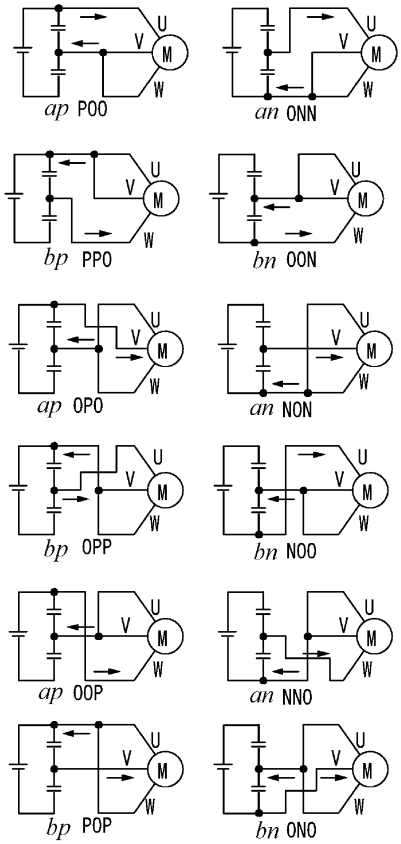

Fig. 3. Illustration of the influence of the small redundant output voltage vectors on the neutral point potential.

In the conventional space-vector PWM approach, the output voltage is generated by utilizing the nearest triangle vectors (NTV) [4], [5]. Among the triangles shown in Fig. 2, NTV is the triangle where the tip point of the reference vector belongs. Utilizing these three voltage vectors, the reference and output volt-seconds are matched every PWM cycle. The time length of

TABLE I
NTV PWM DUTY-CYCLE CALCULATIONS

Region	NTV	Time length of NTV
A1,B1 C1,D1 E1,F1	*op, oo, on*	$t_0 = T\{1-2k\sin(\theta'+\pi/3)\}$
	ap, an	$t_1 = 2kT\sin(\pi/3-\theta')$
	bp, bn	$t_2 = 2kT\sin\theta'$
A2,B2 C2,D2 E2,F2	*ap, an*	$t_1 = 2T\{1-k\sin(\theta'+\pi/3)\}$
	c	$t_3 = 2kT\sin\theta'$
	a	$t_4 = T\{2k\sin(\pi/3-\theta')-1\}$
A3,B3 C3,D3 E3,F3	*ap, an*	$t_1 = T(1-2k\sin\theta')$
	bp, bn	$t_2 = T\{1-2k\sin(\pi/3-\theta')\}$
	c	$t_3 = T\{2k\sin(\theta'+\pi/3)-1\}$
A4,B4 C4,D4 E4,F4	*bp, bn*	$t_2 = 2T\{1-k\sin(\theta'+\pi/3)\}$
	c	$t_3 = 2kT\sin(\pi/3-\theta')$
	b	$t_5 = T(2k\sin\theta'-1)$

each vector is calculated as summarized in Table I. In the table, T is the PWM period, k is the modulation index (magnitude of the reference voltage vector normalized by $Ed/\sqrt{3}$), and θ' is the angle from the nearest "a" voltage vector. The total output time length of the op, oo, and on vectors is t_0. The total output time length of the ap and an vectors is t_1. Likewise, the total output time length of the bp and bn vectors is t_2.

Given the duty cycle of the vectors, the pulse pattern (the vector/switching sequence) is determined with a high waveform quality and a small number of switchings criteria. The popular pulse pattern of the NTV approach that is shown in Fig. 4 [4], [5] is adopted in this paper. In this pattern, from the origin of the hexagon outwards, the number of commutations decreases. The output phase-to-neutral voltages of the internal hexagon (A1–F1) in Fig. 2 are bipolar. Outward from that region, they increasingly become unipolar.

In order to control the neutral point potential, it is necessary to control the duty ratio (the redundancy function) of the two small (redundant) vectors. The redundancy functions are defined in the following:

$$\alpha_1 = \frac{t_{ap}}{t_1}, \qquad t_{ap} + t_{an} = t_1; \quad 0 \le \alpha_1 \le 1 \tag{1}$$

$$\alpha_2 = \frac{t_{bp}}{t_2}, \qquad t_{bp} + t_{bn} = t_2; \quad 0 \le \alpha_2 \le 1. \tag{2}$$

In (1) and (2), t_{ap} and t_{an} are the time lengths of the ap and an vectors, and t_{bp} and t_{bn} are the time lengths of the bp and bn vectors. Therefore, the average neutral current over a PWM cycle i_n can be calculated in the following:

$$i_n = i_X(R)\cdot(t_{an}-t_{ap}) + i_Y(R)\cdot(t_{bp}-t_{bn}) + i_Z(R)\cdot t_3. \tag{3}$$

The variables $i_X(R)$, $i_Y(R)$, and $i_Z(R)$ are the phase current functions defined in Table II. As the table shows, the output voltage vector region determines the phase current functions.

Substituting (1) and (2) in (3), the following is obtained:

$$i_n = i_X(R)\cdot(1-2\alpha_1)\cdot t_1 - i_Y(R)\cdot(1-2\alpha_2)\cdot t_2 + i_Z(R)\cdot t_3. \tag{4}$$

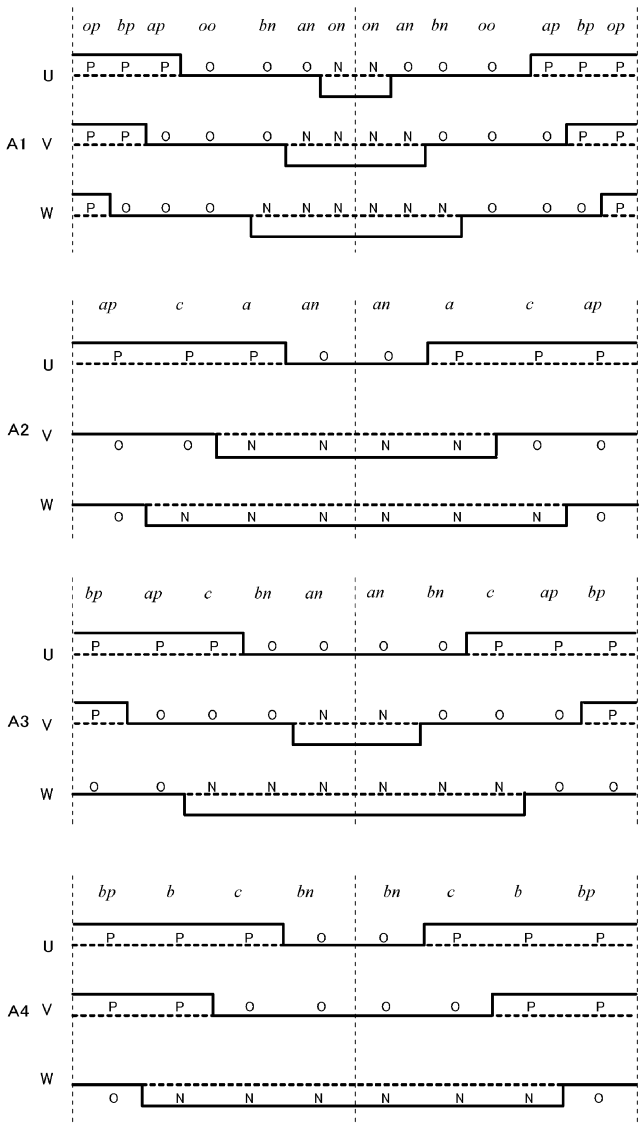

Fig. 4. Pulse pattern of NTV-PWM in A1–A4.

TABLE II
VOLTAGE-VECTOR-REGION-DEPENDENT PHASE CURRENT FUNCTIONS

Region(R)	A	B	C	D	E	F
$i_X(R)$	i_u	i_v	i_v	i_w	i_w	i_u
$i_Y(R)$	i_w	i_w	i_u	i_u	i_v	i_v
$i_Z(R)$	i_v	i_u	i_w	i_v	i_u	i_w

As a result, i_n is determined in each PWM cycle as a function of α_1, α_2, and the phase current functions. Notice that in A1–F1 and A3–F3, two redundancy functions exist, while in A2–F2 and A4–F4 there is only one redundancy function as a consequence of the fact that only one small vector pair is utilized in the NTV approach. It is apparent that when two redundancy functions exist, they can be independently selected to control the neutral potential.

TABLE III
CURRENT POLARITY COORDINATED OPTIMAL REDUNDANCY FUNCTIONS

$i_X(R) \geq 0$	$\alpha_1 = \alpha$
$i_X(R) < 0$	$\alpha_1 = (1-\alpha)$
$i_Y(R) \geq 0$	$\alpha_2 = (1-\alpha)$
$i_Y(R) < 0$	$\alpha_2 = \alpha$

The choice of uniform distribution function ($\alpha_1 = \alpha_2 = \alpha$) results in the following simple analytical formula for the neutral potential current:

$$i_n = (1-2\alpha)\cdot\{i_X(R)\cdot t_1 - i_Y(R)\cdot t_2\} + i_Z(R)\cdot t_3. \quad (5)$$

The first term of (5) shows the neutral point current can be controlled by the redundancy function. Since this control technique utilizes uniform redundancy functions for both (ap, an) and (bp, bn) vectors, the magnitude of the $\{i_X(R)\cdot t_1 - i_Y(R)\cdot t_2\}$ term is dependent on the polarity of $i_X(R)$ and $i_Y(R)$. If they have the same polarity the magnitude becomes small, otherwise, it becomes large. On the other hand, from the neutral potential control perspective it is preferable to have a large magnitude so that the contribution of the small vectors to the neutral current can be varied in a wide range by controlling α. Since the same polarities case corresponds to the near-zero-PF operating condition, such operating points are associated with poor performance. This issue becomes important when the second term in (5) becomes dominant and must be offset by the first term (corresponding to high modulation index output conditions). Under such conditions, even the extremum values of the redundancy function (0 or 1) may not be sufficient to compensate for the influence of the medium voltage vector on the neutral potential. Hence, poor neutral-potential performance. This argument suggests that the uniform redundancy function assumption results in an unnecessary performance constraint and leads to the choice of nonuniform redundancy functions. The above discussion also hints that the key to the success of the nonuniform redundancy function method is to coordinate the redundancy functions with the load current polarity functions.

III. A NOVEL NEUTRAL POINT POTENTIAL STABILIZATION TECHNIQUE

Equation (4) suggests taking the polarity information of the currents $i_X(R)$ and $i_Y(R)$ into account, and then optimizing the two independent redundancy functions so that the widest performance range is obtained. By coordinating the redundancy functions α_1 and α_2 with the polarity of the current functions $i_X(R)$ and $i_Y(R)$ as shown in Table III, the maximum charge range for neutral potential control becomes available. Then, with the appropriate choice of the new common variable α the neutral current and the neutral potential can be controlled.

To illustrate the difference between (5) and the proposed method, the following cases are considered. For instance, in the first sector of the voltage hexagon (region A in Fig. 2), 1, 0 (lagging), and -1 PF conditions correspond to the phase current polarity information shown in Table IV.

TABLE IV
PHASE CURRENT POLARITY AS A FUNCTION OF PF IN REGION A

PF	1	0	–1
$i_X(A) = i_u$	+	+	–
$i_Y(A) = i_w$	–	+	+
$i_Z(A) = i_v$	– or +	–	+ or –

In (5), regardless of the the PF, the neutral current is calculated in the following:

$$i_n = (1-2\alpha)\cdot(i_u\cdot t_1 - i_w\cdot t_2) + i_v\cdot t_3. \quad (6)$$

For the proposed current polarity coordinated redundancy function method, however, the neutral current formula is calculated differently for each PF condition. For PF values of 1, 0, and -1, the neutral current is calculated, respectively, in the following:

$$i_n = \left\{ \begin{array}{ll} (1-2\alpha)\cdot(i_u\cdot t_1 - i_w\cdot t_2) + i_v\cdot t_3, & PF = 1 \\ (1-2\alpha)\cdot(i_u\cdot t_1 + i_w\cdot t_2) + i_v\cdot t_3, & PF = 0 \\ (1-2\alpha)\cdot(-i_u\cdot t_1 + i_w\cdot t_2) + i_v\cdot t_3, & PF = -1 \end{array} \right\}. \quad (7)$$

Comparing (6) to (7), it becomes obvious that the proposed method provides a larger controllable charge range for neutral point potential control. In particular, for the zero-PF case, $(i_u\cdot t_1 - i_w\cdot t_2)$ is small while for the proposed method $(i_u\cdot t_1 + i_w\cdot t_2)$ is large and results in a wider control range. As this example illustrates, the neutral point potential can be better controlled with the proposed method. Note that, based on the same observation, for the proposed method, (4) can be rewritten in the following:

$$i_n = (1-2\alpha)\cdot(|i_X(R)|\cdot t_1 + |i_Y(R)|\cdot t_2) + i_Z(R)\cdot t_3. \quad (8)$$

The above equation indicates that in the proposed method the redundant voltage vectors can be efficiently utilized to control the neutral point current. From this equation for a given reference neutral current value, the corresponding α can be easily calculated.

IV. NEUTRAL POTENTIAL PERFORMANCE COMPARISON BETWEEN THE PROPOSED AND POPULAR METHODS

In this section, the neutral potential performance of the proposed method will be compared to the popular scalar methods by means of analysis and computer simulations. In particular, the scalar unipolar modulation technique is compared to the proposed method due to its popularity and established neutral potential control technique [3]. As the unipolar and bipolar modulation techniques are both scalar techniques, from here on, when discussing these methods, the term "scalar" will be omitted for the sake of simplicity.

In the space-vector modulation technique, for a selected set of voltage vectors and a specific switching sequence, the pulse pattern is completely defined. This pulse pattern can also be generated with a scalar modulation technique. In the unipolar modulation technique, two triangular carrier waves are compared with the reference voltage modulation wave of a phase to generate the switching pattern of the associated inverter leg [3],

TABLE V
REDUNDANCY FUNCTIONS OF THE UNIPOLAR MODULATION

Mode I	$0 \le \alpha_1 \le 1,\ \alpha_2 = 0$
Mode II	$\alpha_1 = 1, 0 \le \alpha_2 \le 1$

[14]. The intersections define the switching instants. This approach naturally results in unipolar phase-to-neutral output voltages within each PWM cycle and throughout the whole inverter voltage hexagon. In the bipolar modulation technique [14], one triangular carrier wave is compared with two modulation waves per phase. The intersection points define the switching instants. When the reference voltage magnitude is small (corresponding to the region in A1–F1) the output voltages are bipolar, and at higher magnitudes where modulation waves saturate, they increasingly become unipolar.

The above discussion indicates that at low modulation (corresponding to the A1–F1 hexagon) the pulse pattern of the bipolar modulation technique is the same as the NTV pattern. Similarly, at higher modulation levels (outside the A1–F1 hexagon), the NTV pattern approaches the unipolar modulation pattern. In A2–F2 and A4–F4, the pulse pattern of unipolar modulation is the same as the NTV pattern. In the A3–F3 triangles, two phases have unipolar and one phase has bipolar pattern. Note that the pulse pattern (the switching sequence) in each scalar modulation is exactly equivalent to an NTV pattern. On the other hand, the width of the pulses may differ as a function of the modulation parameters involved. Finding the exact mathematical relations between the scalar modulation techniques and the NTV method is beyond the scope of this paper. However, in the following, we employ the pulse sequence equivalency of scalar and vector methods in order to quantitatively obtain the neutral current control boundaries of the scalar methods.

In the unipolar modulation case, when at least two out of the three phase modulation signals are positive, the pulse pattern becomes equivalent to NTV with one of the redundancy functions fixed to zero while the other is variable. This defines Mode I in Table V. When at least two out of the three modulation signals have negative sign, the pulse pattern becomes equivalent to NTV with one redundancy function equal to one (100% duty cycle) and the other a variable. This case defines Mode II and the modes are summarized in Table V. Either one of the two modes with specific redundancy function value can be created by adding a zero-sequence signal to the modulation signals [3]. Comparing the NTV with fully controllable two redundancy functions to the unipolar modulation with one redundancy function fixed and the other variable, it becomes obvious the neutral current control range of the unipolar modulation technique is smaller.

In the bipolar modulation technique, the pulse pattern is the same as the NTV approach. Therefore, both redundancy functions α_1 and α_2 exist and they are variable. As a result, it can be concluded that the bipolar modulation technique results in a wider neutral current control range/capability compared to the unipolar modulation technique. However, a method of varying the redundancy functions independently or in a coordinated manner is not evident from the modulation signals. Therefore, it appears that the space-vector approach with the NTV pattern is not only preferable from the neutral potential performance perspective, but it is also insightful and easy to implement.

The performance of the unipolar modulation and the space-vector NTV approach with the proposed neutral potential control method are compared by means of computer simulations. In the unipolar modulation technique, the neutral current/potential is controlled by adding a zero-sequence signal to all the three phase modulation waves [3]. A method to calculate the zero-sequence signal that minimizes the neutral potential error is described in [3]. In this paper, for the purpose of comparison, the neutral potential behavior of the unipolar modulation will be investigated via the redundancy functions that correspond to the zero-sequence signal. Therefore, in the simulation, the constraints of Table V will be recognized when selecting the redundancy function of the unipolar modulation technique.

For the sake of simplicity, a reduced model of the NPC three-level inverter drive is employed in the simulation. The system average model over a PWM cycle (T) is employed. Therefore, only the average value of the neutral current, modulation signals, etc., is calculated. The load is represented with a balanced three-phase sinusoidal current source. Assuming a condition that results in an unbalance between the upper and lower capacitor has occurred, a reference neutral current with the average value of i_n^* is necessary to regulate the neutral potential. In the unipolar modulation method case, the relation between i_n^* and the corresponding redundancy functions can be calculated from (4) for Mode I of Table V in the following:

$$\alpha_{1MI} = \frac{1}{2}\left(1 - \frac{i_n^* + i_Y(R)\cdot t_2 - i_Z(R)\cdot t_3}{i_X(R)\cdot t_1}\right) \tag{9}$$

$$\alpha_{2MI} = 0. \tag{10}$$

Likewise, for Mode II the redundancy functions are calculated in the following:

$$\alpha_{1MII} = 1 \tag{11}$$

$$\alpha_{2MII} = \frac{1}{2}\left(1 - \frac{i_n^* - i_X(R)\cdot t_1 - i_Z(R)\cdot t_3}{i_Y(R)\cdot t_2}\right). \tag{12}$$

In the proposed method the common redundancy function is calculated from (8) as follows:

$$\alpha = \frac{1}{2}\left(1 - \frac{i_n^* - i_Z(R)\cdot t_3}{|i_X(R)|\cdot t_1 - |i_Y(R)|\cdot t_2}\right). \tag{13}$$

Given the fact that the redundancy functions are limited to values between 0–1, the realizable neutral current can be smaller than the reference value. If (9), (12), and (13) give unfeasible redundancy function values, the realizable neutral current can be recalculated from the same equations with the boundary values of the redundancy functions. While in the proposed method the optimal redundancy function is calculated from (13), in the unipolar modulation method, the optimal value (that corresponds to the optimal zero-sequence signal) is determined by comparing the results of Mode I and II. The mode that results in a smaller error between the reference and realizable neutral current values is the optimal solution of unipolar modulation.

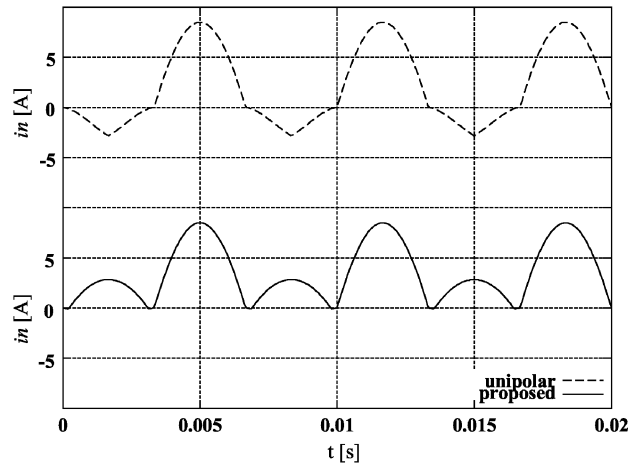

Fig. 5. Realizable neutral current in the unipolar modulation method (top) and the proposed method with optimal redundancy function (bottom).

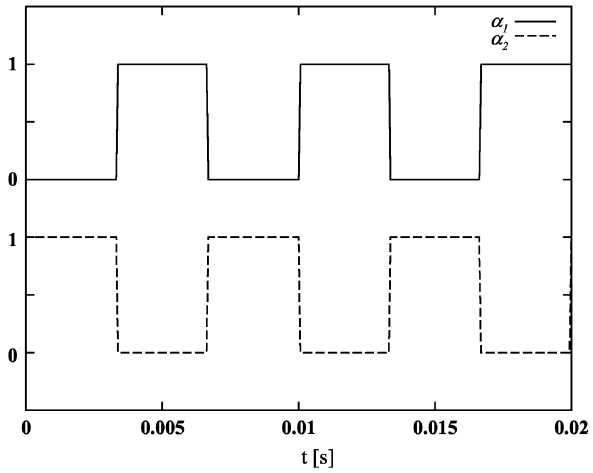

Fig. 7. Redundancy functions of the proposed method $(k = 0.6)$.

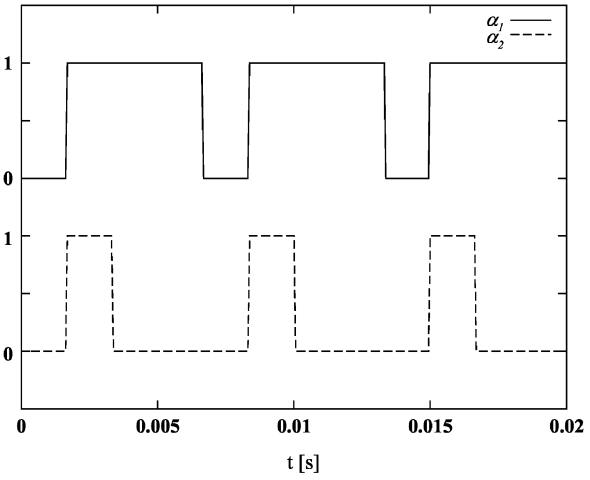

Fig. 6. Redundancy functions of the unipolar modulation method $(k = 0.6)$.

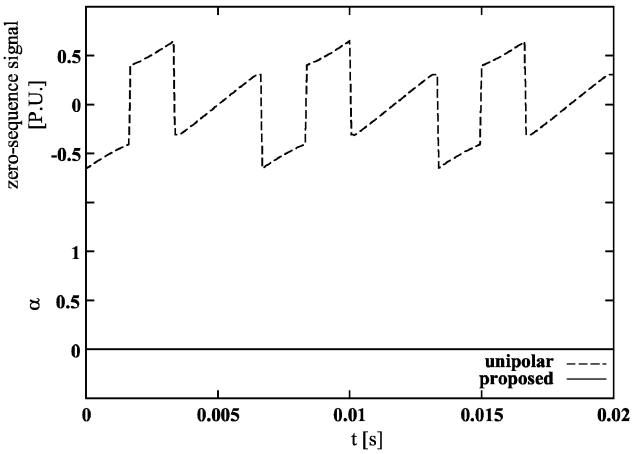

Fig. 8. Zero-sequence signal of the unipolar modulation method (top) and the common redundancy variable of the proposed method (bottom).

In the simulation study, first the unipolar modulation method with zero-sequence signal injection and the proposed method are compared from the neutral current capability perspective. The zero-PF (lagging) condition is investigated as the worst PF condition. A three-phase Y-connected sinusoidal-current-source-type load with 10 A (rms, per phase) and 50 Hz is considered. The operating modulation index is $k = 0.6$ (corresponding to A2–A3–A4, B2–B3–B4... regions), and a neutral current reference value of 10 A (positive dc current with constant magnitude) case is considered. Since the reference neutral current magnitude is large, the redundancy functions of both methods are expected to be saturated (0 or 1) and 10-A neutral current is not realizable. However, as shown in Fig. 5, the difference between the realizable and reference neutral current values is smaller in the proposed method. Figs. 6 and 7 show the redundancy functions corresponding to each case. In the unipolar modulation case, one of the redundancy functions is constrained to a boundary value as in Table V, and the other is controllable. The two redundancy functions cannot always be stretched to their extreme values simultaneously. In the proposed method, during saturation, both functions are stretched to their extreme values simultaneously. Comparing the two figures, it becomes obvious that in the unipolar modulation method the neutral current is smaller due to the fact that there is only one controllable redundancy function. In the proposed method, both variables can be operated at the saturation limits so that the maximum possible current is obtained. Both neutral current waveforms of Fig. 5 have a frequency equal to three times the output frequency of the inverter. This is due to the fact that at $k = 0.6$ the medium voltage vector is utilized and it loads the neutral point at three times the output frequency.

In Fig. 8, the common redundancy variable of the proposed method and the zero-sequence signal of the unipolar modulation method are illustrated. Varying in a wide range, the zero-sequence signal does not give intuition about the occurring saturation condition. The common redundancy variable of the proposed method, on the other hand, clearly demonstrates the saturation condition. A value of zero (minimum) or one (maximum) indicate that the variable is at its saturation level and there is not enough charge to immediately and completely compensate for the neutral potential unbalance. Furthermore, a value of 0.5 implies balanced (zero) neutral potential condition while a deviation from this value implies that an unbalance exists. The

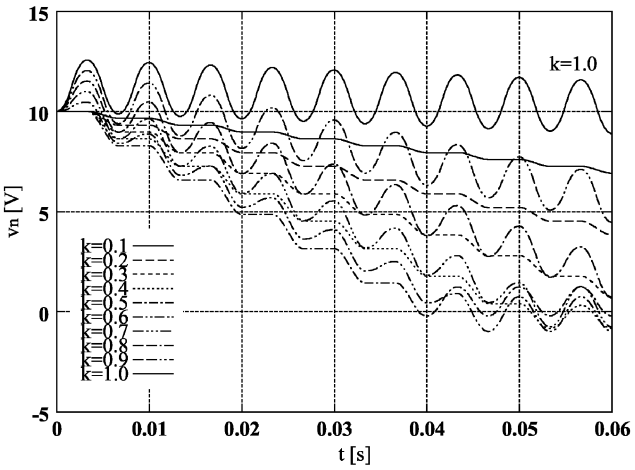

Fig. 9. Neutral potential control behavior of the unipolar modulation method for various modulation index values.

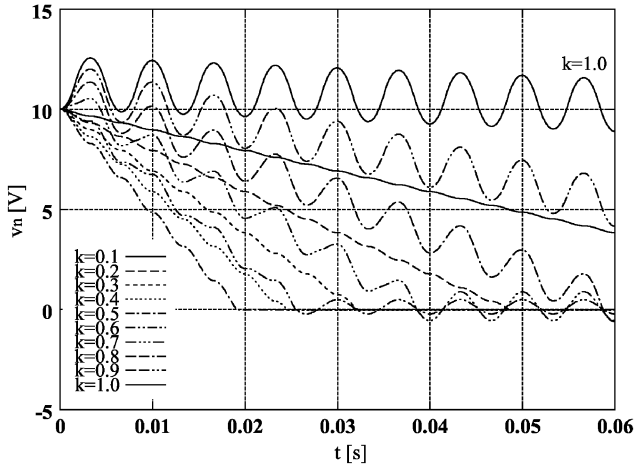

Fig. 10. Neutral potential control behavior of the proposed method for various modulation index values.

amount and direction of the deviation from 0.5 gives hints about the direction and magnitude of the neutral potential deviation. Therefore, the proposed method is highly intuitive.

In the second stage of the computer simulation study, the neutral potential regulation capability of the proposed method and the unipolar modulation method are demonstrated in detail. The dc link of the NPC consists of two 4500-μF capacitors connected in series. An initial neutral potential offset value of 10 V is assumed. The load is the previously described three-phase current source with 10-A rms and 50 Hz. The zero-PF (lagging) condition is considered as the worst operating point. The reference neutral current is set as 14 A (equal to the peak value of the output current). As long as the neutral potential error exists, the controller attempts to generate the 14-A neutral current so that the error decreases. When the error becomes zero, the controller is disabled and the redundancy function is set to 0.5 value. The performance is tested for various modulation index values in both the unipolar modulation method and the proposed method. The simulation waveforms are shown in Figs. 9 and 10.

Comparing Figs. 9 and 10, it can be observed that at modulation indices below 0.8 the performance of the proposed method is superior to the unipolar modulation method. In the proposed method, the neutral potential approaches the zero level more rapidly than the unipolar modulation method. At low modulation, for example at $k = 0.5$, the proposed method is approximately twice as fast as the unipolar modulation method. This is due to the fact that the redundancy function of the unipolar modulation method is not coordinated with the output current polarities and half of the capability is lost compared to the proposed method. However, at higher modulation indexes, the difference disappears due to the fact that the time length of the small vectors and their neutral current regulation capability becomes negligible and the medium vector becomes highly dominant.

At very low modulation (near zero modulation index) although the proposed method has twice as fast compensation speed as the unipolar method, the compensation time is quite long and rapidly increases as the zero modulation index is approached. This is due to the fact that at very low modulation the zero voltage vectors are dominant and the small vectors that compensate for the neutral potential error have a very small time length. However, it is practically not very likely that a large neutral potential drift will occur at very low modulation index. Therefore, the long compensation time of the very low modulation range is not a problematic characteristic. On the other hand, at higher modulation indices as the neutral potential drift is likely to occur, the compensation capability of the proposed method is necessary and beneficial. Detailed observation of Fig. 10 suggests that the advantage range of the proposed method is 0.2–0.8 modulation index.

In both the proposed method and the unipolar modulation method, the largest neutral voltage ripple occurs at the full modulation index $(k = 1.0)$. This operating point is typically selected as the dc-bus capacitor design point of a general-purpose inverter drive. Based on the capacitor voltage ripple tolerance value selected (typically 1%–3%), the capacitance value can be analytically calculated. Then, depending on the input rectifier characteristics (diode bridge or PWM rectifier), the inverter load current characteristics, and the modulation technique involved, the dc-bus capacitor ripple current rms value is calculated. Finally, commercially available capacitors that meet both criteria are evaluated. If the capacitors with the calculated capacitance value do not meet the ripple current rating criteria, then the capacitor size is increased until this condition is met. Under such rare conditions, the voltage ripple becomes smaller than the tolerance value specified at the initial stage but the size and the cost of the drive increase.

With the design criteria for both the proposed and the unipolar modulation method being the same, it becomes obvious that the proposed method does not reduce the capacitor size. However, with the same capacitor size, the proposed technique results in better performance in the 0.2–0.8 modulation index range. In order to obtain low neutral potential variation beyond 0.8 modulation index, it is possible to modify the NTV PWM pulse pattern and reduce the duty cycle of the medium voltage vector such that the ripple due to the medium voltage vector is decreased. However, the pulse pattern approaches the two-level inverter pulse pattern and the current ripple rapidly increases such that

the advantages of the NPC three-level-inverter are lost. Details of such techniques are beyond the scope of this paper and will be addressed in a future paper.

V. Experimental Results

The feasibility of the proposed method has been proven via laboratory experiments. In the experiments, an induction motor with 7.5-kW, 1750-min^{-1}, 400-V, and 15.2-A ratings is driven from a PWM-NPC inverter. The induction motor has no mechanical load and, therefore, its PF for this operating condition is poor (near zero). The NPC three-level inverter is operated in the constant-volts-per-hertz mode and the slope of the V/f curve is selected such that at 60-Hz output, unity modulation index $(k = 1)$ is obtained. The inverter dc bus consists of two capacitors in series with 4500 μF each. The carrier frequency is 8 kHz.

The neutral potential controller of the experimental system is designed with the low-cost criteria and employs a naive form of the proposed control technique. The neutral potential feedback information to the controller is obtained via two comparators with binary output (B1 and B2). If the neutral potential is above the tolerance band value ΔV, the first comparator output becomes high (B1 = H). Otherwise it becomes low (B1 = L). If the neutral potential is below $-\Delta V$, then the second comparator output becomes high (B2 = H). Otherwise, it is low (B2 = L). Therefore, two binary signals B1–B2 can have the logic values of HL, LL, or LH each representing a zone in the tolerance band of the neutral potential controller. If B1 is high, then α is increased and if B2 is high, then α is decreased in increments defined by the selected time constant of a first-order linear low-pass filter (in the experiment, it is 1 ms). If both B1 and B2 are low, then α is incremented (or decremented) with the same time constant until it returns to 0.5. Given α, the redundancy functions α_1 and α_2 are distributed according to the proposed method. This approach provides satisfactory performance and eliminating an expensive voltage isolator and multibit analog-to-digital converter results in cost and size reduction.

In the experiment, the tolerance band of the neutral potential was selected as 10 V. The front end consists of a three-phase diode rectifier and the dc-bus voltage is 560 V. The half-rated-speed operating point ($f_{\text{out}} = 30$ Hz, $k = 0.5$) was chosen to demonstrate the performance of the experimental system. An initial neutral potential deviation of 10 V was created by intentionally disabling one of the two binary neutral potential feedback signals and biasing the tolerance band. Following, the feedback signal was enabled and the tolerance bias was removed. Then, the performance of the proposed controller could be tested. The regulation capability of the proposed method is demonstrated in Fig. 11 in detail. As the controller is activated, the redundancy function decreases with the 1-ms time constant and saturates at zero level in order to rapidly return the neutral potential from the initial value of 10 V to 0 V. Once the error is corrected, the redundancy function returns to the normal value of 0.5 again with the 1-ms time constant. The regulation is completed in less than one output cycle, and during this transient the neutral current has a positive average value that indicates the full neutral current capacity is efficiently utilized.

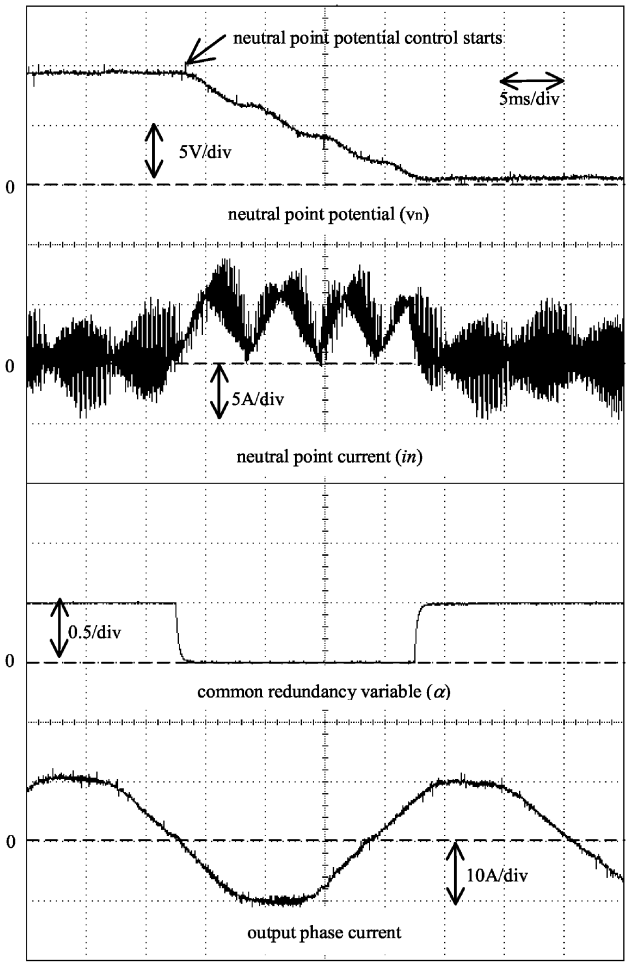

Fig. 11. Experimental waveforms of the proposed method $(k = 0.5)$. Top to bottom: neutral point potential, neutral current, α, and output phase current.

VI. Conclusions

A novel neutral point potential control technique has been reported. Utilizing the polarity information of the phase currents, the method efficiently distributes the redundant voltage vectors to maintain small neutral current and easily control the neutral point potential. Detailed analysis investigates the neutral potential behavior of the proposed and the popular methods and computer simulations demonstrate the capability of the proposed method. The feasibility of the proposed method has been proven via laboratory experiments. Furthermore, a low-cost implementation of the control technique has been shown to provide satisfactory performance. Therefore, the economical feasibility of the general-purpose NPC three-level inverter in low-voltage drive applications has been strengthened and its application range widened.

References

[1] A. Nabae, I. Takahashi, and H. Akagi, "A new neutral-point-clamped PWM inverter," *IEEE Trans. Ind. Applicat.*, vol. 17, pp. 518–523, Sept./Oct. 1981.

[2] Yaskawa Electric Corp. [Online]. Available: http://www.yaskawa.co.jp
[3] S. Ogasawara and H. Akagi, "Analysis of variation of neutral point potential in neutral point clamped voltage source PWM inverters," in *Conf. Rec. IEEE-IAS Annu. Meeting*, 1993, pp. 965–970.
[4] T. Kawabata, M. Koyama, S. Tamai, T. Fujii, and R. Uchida, "A new PWM method of a three-level inverter considering minimum pulse width and neutral voltage balance control," *Trans. Inst. Elect. Eng. Jpn.*, vol. 113-D, no. 7, pp. 865–873, 1993.
[5] M. Koyama, T. Fujii, R. Uchida, and T. Kawabata, "Space voltage vector based new PWM method for large capacity three-level GTO inverter," in *Proc. IEEE IECON'92*, 1992, pp. 271–276.
[6] T. Kudor and K. Shimane, "A suppression method of neutral potential variations for 3-level inverter," in *Conf. Rec. IEEJ-IAS Annu. Meeting*, 1995, pp. 187–190.
[7] M. Ichihara, T. Akiyama, J. Shimomura, K. Tamura, and M. Terashima, "Control method of the neutral point voltage of NPC inverter connected to utility lines," in *Conf. Rec. IEEJ-IAS Annu. Meeting*, 1995, pp. 197–200.
[8] J. Steinke, "Switching frequency optimal PWM control of a three-level inverter," in *Proc. EPE'89*, 1989, pp. 1267–1272.
[9] Y. Tadros, S. Salama, and R. Hof, "Three level IGBT inverter," in *Proc. IEEE PESC'92*, 1992, pp. 46–52.
[10] N. Celanovic and D. Borojevic, "A comprehensive study of neutral-point voltage balancing problem in three-level neutral-point-clamped voltage source PWM inverters," *IEEE Trans. Power Electron.*, vol. 15, pp. 242–249, Mar. 2000.
[11] C. Newton and M. Sumner, "Neutral point control for multi-level inverters: Theory, design, and operational limitations," in *Conf. Rec. IEEE-IAS Annu. Meeting*, 1997, pp. 1336–1343.
[12] D. H. Lee, S. R. Lee, and F. C. Lee, "An analysis of midpoint balance for the neutral-point-clamped three-level VSI," in *Proc. IEEE PESC'98*, 1998, pp. 193–199.
[13] K. Yamanaka, A. M. Hava, H. Kirino, Y. Tanaka, M. Zenke, and N. Koga, "A novel neutral point potential stabilization technique using information of output voltage vector and currents," in *Conf. Rec. ICEE*, 2000, pp. 717–720.
[14] B. Velaerts, P. Mathys, and G. Bingen, "New developments of 3-level PWM strategies," in *Proc. EPE'89*, 1989, pp. 411–416.
[15] F. Wang, "Sine-triangle vs. space vector modulation for three-level PWM voltage source inverters," in *Conf. Rec. IEEE-IAS Annu. Meeting*, 2000, pp. 2482–2488.
[16] H. Kim, D. Jung, and S. Sul, "A new discontinuous PWM strategy of neutral-point clamped inverter," in *Conf. Rec. IEEE-IAS Annu. Meeting*, 2000, pp. 2017–2023.

Katsutoshi Yamanaka received the B.S. and M.S. degrees in electrical engineering from Kyushu University, Fukuoka, Japan, in 1991 and 1993, respectively.

In 1993, he joined Yaskawa Electric Corporation, Kitakyushu, Japan. His research interests include power electronics and motor drives.

Mr. Yamanaka is a member of the Institute of Electrical Engineers of Japan.

Ahmet M. Hava (S'91–M'98) was born in Mardin, Turkey, in 1965. He received the B.S. degree from Istanbul Technical University, Istanbul, Turkey, in 1987, and the M.S. and Ph.D. degrees from the University of Wisconsin, Madison, in 1991 and 1998, respectively, all in electrical engineering.

In 1995, he was with Rockwell Automation-Allen Bradley Company, Mequon, WI. From 1997 to 2002, he was with Yaskawa Electric America, Inc, Waukegan, IL. He is presently an Assistant Professor at the Middle East Technical University, Ankara, Turkey. His research interests include power electronics, electric machines, and control.

Hiroshi Kirino was born in Kagoshima, Japan, in 1967. He graduated from the Sendai Polytechnic College, Sendai, Japan, in 1988.

In 1988, he joined Yaskawa Electric Corporation, Kitakyushu, Japan, where he is currently developing a general-purpose inverter.

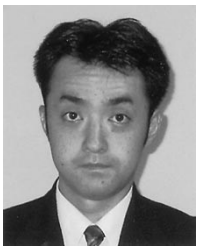

Yoshiyuki Tanaka received the B.S. degree in mechanical and electrical systems engineering from Kurume National College of Technology, Kurume, Japan, in 1996, and the M.S. degree in electrical engineering from Nagaoka University of Technology, Nagaoka, Japan, in 1998.

In 1998, he joined Yaskawa Electric Corporation, Kitakyushu, Japan. His research interests include power electronics and motor drives.

Mr. Tanaka is a member of the Institute of Electrical Engineers of Japan.

Noritaka Koga received the B.S. degree in control engineering from Kyushu Institute of Technology, Kitakyushu, Japan, in 1983.

In 1983, he joined Yaskawa Electric Corporation, Kitakyushu, Japan. He took part in the development of general-purpose transistor (IGBT) PWM inverters, in particular, in the power electronics field. In 1991, he joined Yaskawa Electric Europe GmbH, Schwalbach, Germany. He returned to Yaskawa Electric Corporation, Japan, in 1995, where he has worked on the development of general-purpose inverters.

Tsuneo (Joe) Kume (M'68) received the B.S. degree from Waseda University, Tokyo, Japan, in 1960, and the M.S. and Ph.D. degrees from the University of Missouri, Columbia, in 1968 and 1970, respectively, all in electrical engineering.

In 1960, he joined Yaskawa Electric Corporation, Kitakyushu, Japan. In 1966, he began a leave of absence to study at the University of Missouri. After returning to Yaskawa Electric, he developed the first commercially produced general-purpose transistor PWM inverter. He also played key roles in developing the vector-controlled transistor inverter in 1979, which was successfully applied to drive systems in various fields, such as machine tools and in the iron and steel industry. He moved to the U.S. in 1996 to join Yaskawa Electric America, Inc., Waukegan, IL, as Director of R&D, where he continues his activities in the field of power electronics and motor drives.

Dr. Kume is a member of the Institute of Electrical Engineers of Japan.